Chinese Chemical Letters 32 (2021) 2108–2116

Contents lists available at ScienceDirect

Chinese Chemical Letters

journal homepage: www.elsevier.com/locate/cclet

Review

Advances in engineering RuO_2 electrocatalysts towards oxygen evolution reaction

Cheng Wang[a], Liujun Jin[a], Hongyuan Shang[a], Hui Xu[a,*], Yukihide Shiraishi[b], Yukou Du[a,*]

[a] College of Chemistry, Chemical Engineering and Materials Science, Soochow University, Suzhou 215123, China
[b] Department of Applied Chemistry, Sanyo-Onoda City University, Sanyo-Onoda, Yamaguchi 756-0884, Japan

ARTICLE INFO

Article history:
Received 11 September 2020
Received in revised form 30 October 2020
Accepted 24 November 2020
Available online 1 December 2020

Keywords:
RuO_2
Oxygen evolution reaction
Electrocatalysts
Water electrolysis
Catalysis

ABSTRACT

Water electrolysis technology holds the perfect promise of the hydrogen production, yet control of efficiency and rate of water electrolysis greatly relies on the availability of high-performance electrode materials for kinetic-sluggish oxygen evolution reaction (OER). Accordingly, substantial endeavors have been made to explore advanced electrode materials over the past decade. Recently, RuO_2 and RuO_2-based materials have been demonstrated to be promising for OER due to their remarkable electrocatalytic activity and pH-universal application. Herein, the great achievements and progresses of this flourishing spot are comprehensively reviewed, which are started by a general description of OER to understand the reaction mechanism in detail. Subsequently, the key advantages and issues of RuO_2 towards OER are also introduced, followed by proposing many advanced strategies for further promoting the electrocatalytic OER performance of RuO_2. Finally, the daunting challenges and future progresses of RuO_2 electrocatalysts toward practical water oxidation are highlighted, aiming to provide guidance for the fabrication of desirable RuO_2-based electrocatalysts toward OER.

1. Introduction

Oxygen evolution reaction (OER) plays a crucial role in energy conversion systems, including metal-air battery, water splitting, CO_2 reduction, and so on [1–4]. Essentially, the OER commonly undergoes a four electron and proton transfer process, leading to sluggish reaction kinetics and demanding a higher energy to overcome the kinetic barrier and overpotential [5–8]. In this regard, substantial research efforts have been made to the fabrication of highly efficient OER electrocatalysts with both enhanced reaction kinetics and durability in alkaline media, such as transition metal composites, perovskites, and carbon-based composites [9–19]. Despite these electrocatalysts are highly active and stable in alkaline conditions, they are also kinetic-sluggish and unstable in acidic solution [20–23]. Generally, OER electrocatalysis in acidic solution is more preferable as compared to alkaline media since acidic electrolyte has much higher ionic conductivity [24–26]. To this end, exploring efficient OER electrocatalysts with enhanced kinetic and durability under both alkaline and acidic media is highly appreciated. Among various electrocatalysts, Ru has been widely researched due to its high intrinsic OER activity and relatively lower cost as compared to other precious metals [27,28]. Currently, rutile-structured Ru and Ir oxides are well known as the two best electrocatalysts for OER in both alkaline and acidic media [29–33]. In the acidic conditions, it is also well known that RuO_2 can exhibit much higher catalytic activity than IrO_2, while it is unstable because of the formation of soluble RuO_4 at anodic potential. Therefore, tremendous endeavors have been made to the design and development of highly efficient RuO_2 catalysts with great success, and many effective strategies have thus been well developed, such as morphology design, electronic structure engineering, defect engineering, enhancing conductivity, and heterostructure engineering [34–40]. Nonetheless, a comprehensive summary on RuO_2 electrocatalysts for OER is still lacking.

Given the great promise of RuO_2 for OER and exploring more efficient OER electrocatalysts, we herein focus on the recent advances of RuO_2 materials for OER electrocatalysis. First of all, the OER mechanisms in electrolytes under alkaline and acidic media are briefly introduced. Then, the key advantages and aroused challenges of RuO_2 for future applications are also highlighted. The sight into the reaction mechanism and nature of superb performance could boost the further development of more efficient RuO_2-based electrocatalysts. Subsequently, many advanced strategies for further enhancing the electrocatalytic OER performance

* Corresponding authors.
E-mail addresses: ndxuhui006@gmail.com (H. Xu), duyk@suda.edu.cn (Y. Du).

https://doi.org/10.1016/j.cclet.2020.11.051
1001-8417/

of RuO_2 from the perspective of geometric morphology design, crystal facet engineering, electronic structure, defect, conductivity, and heterostructure engineering have also been summarized. Lastly, a cross summary of RuO_2-based electrocatalysts and future envision are systematically discussed to boost the development and better design of RuO_2 electrocatalysts. Through the discussions in this review, we are highly expected to provide some points of view on further promoting the electrocatalytic OER performance of RuO_2 and boosting the rapid development of clean energy technologies.

2. Characterizations of RuO_2 catalysts in oxygen evolution reaction

2.1. Fundamental of oxygen evolution reaction

Efficient OER plays a crucial role in determining the rate and efficiency of various electrochemical reactions due to the unique four electron transfer process, such as rechargeable metal-air batteries and water splitting [41–46]. The possible reaction mechanisms of OER in alkaline/acidic solutions are illustrated in Scheme 1, and the detailed reaction steps are also descripted as follows:

Alkaline solutions (reactions 1–6):

Overall reaction: $4OH^- \rightarrow O_2 + 2H_2O + 4e^-$ (1)

Intermediate reaction steps: $OH^- \rightarrow OH^* + e^-$ (2)

$OH^* + OH^- \rightarrow O^* + H_2O + e^-$ (3)

$2O^* \rightarrow O_2$ (4)

$O^* + OH^- \rightarrow OOH^* + e^-$ (5)

$OOH^* + OH^- \rightarrow O_2 + H_2O + e^-$ (6)

Acidic and neutral solutions (reactions 3, 4, 7–10):

Overall reaction: $2H_2O \rightarrow O_2 + 4H^+ + 4e^-$ (7)

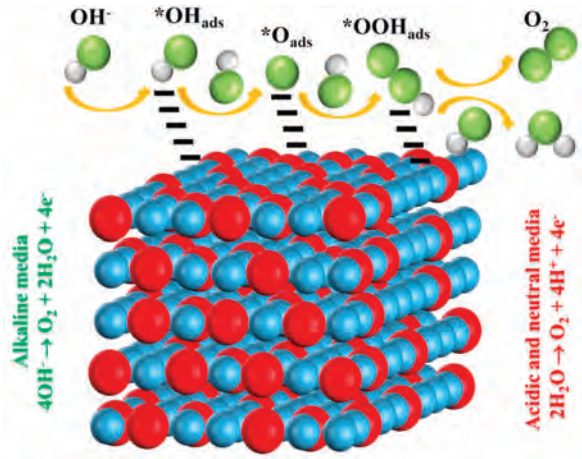

Scheme 1. Scheme of the OER mechanism based on RuO_2 in wide pH values.

Intermediate reaction steps: $H_2O \rightarrow OH^* + H^+ + e^-$ (8)

$OH^* + OH^- \rightarrow O^* + H_2O + e^-$ (3)

$2O^* \rightarrow O_2$ (4)

$O^* + H_2O \rightarrow OOH^* + H^+ + e^-$ (9)

$OOH^* + H_2O \rightarrow O_2 + H^+ + e^-$ (10)

According to the possible reaction mechanisms, it is clearly found that the OH^*, O^* and OOH^* intermediates are generated in sequence [47–56]. In the alkaline conditions, the abundant hydroxyls could effectively boost the generation of OH^* and O^*. After that, the OER process proceeds the direct combination of O^* to form O_2 or further generating OOH^* to release O_2 [16,57–64]. In contrast, there are no hydroxyls ions in the acidic and neutral solutions, which thus demand additional energy to boost the cleavage of covalent bond of H_2O molecule [47,51,65–69]. Of note, the electrocatalytic OER activity of a catalyst is governed by the step with the maximum energy barrier, namely, rate-determining step (RDS) [70,71]. And each step has been demonstrated to exhibit a close relationship in energy barrier, in which the total energy demanded for the transformations from OH^* to O^* and O^* to OOH^* are 3.2 eV. Therefore, a catalyst with an equal energy barrier for the processes of OH^* to O^* and O^* to OOH^* would require the lowest overpotential for driving OER.

2.2. Key advantages of RuO_2 towards OER

According to the proposed mechanism, the electrocatalytic OER activity of is correlated with the energy barriers of transformations of OH^* to O^* and O^* to OOH^*, in which a catalyst with an equal energy barrier for above two processes could exhibit high kinetics [32,57,72]. Bear this consideration into mind, substantial endeavors have been made for realizing the activity promotion of electrocatalysts, and a variety of nonprecious metal-based electrocatalysts have been successfully developed. Despite the numerous efforts devoted, the electrocatalytic OER performance of nonprecious catalysts is still far away from the performance of RuO_2-based electrocatalysts. RuO_2 is well demonstrated to be the most efficient catalyst with an optimal oxygen binding energy close to the top of volcano plot, which is even surpassing than state-of-the-art IrO_2 catalyst. Normally, RuO_2 approaches the top of OER volcano plot from the weak oxygen binding branch, and theoretical studies reveal that the enhancements can be realized by slightly increasing the oxygen adsorption of RuO_2, namely, promoting the capability of binding oxygen intermediates [73,74]. Apart from the higher activity than IrO_2, RuO_2 has also been demonstrated to be much cheaper than IrO_2. In addition, RuO_2 is not only highly active in alkaline conditions but also acidic solution, which could thus be widely employed for industrial water splitting. Furthermore, the Ru atoms have been recently proved to possess suitable adsorption energies for adsorbed oxygen (O_{ads}) and hydrogen (H_{ads}), which could thus display great promise for water electrolysis.

2.3. Key issues of RuO_2 towards OER

Despite the superior activity, the commercial application of RuO_2 toward OER is also greatly hindered by the serious durability issue. Generally, RuO_2 is unstable due to the dissolution from the accompanying over-oxidation at the potential of 1.39 V. And the

specific oxidation reaction can be clearly illustrated as following equation: $RuO_2 + 2H_2O \rightarrow RuO_4$ (aq) + $4H^+ + 4e^-$ ($U^0 = 1.39$ V *vs.* RHE) [75]. Although the unique electronic properties enable the RuO_2 to bind oxygen intermediates moderately to endow them with high electrocatalytic performance toward OER in acidic solution. Previous works have demonstrated that the OER activity and stability of RuO_2 electrocatalyst are much lower than that in alkaline media. Hence, elaborate design of the highly active RuO_2-based electrocatalysts toward acidic OER is highly expected. Apart from the acidic and basic OER, the electrocatalytic performance of RuO_2-based electrocatalysts in neutral conditions still cannot meet the industrial standard. In order to realize the practical application, more research efforts should be devoted to improving the electrocatalytic activity and durability of RuO_2-based electrocatalysts under neutral conditions.

3. Advanced strategies for promoting electrocatalytic OER performance of RuO_2

Although RuO_2 showed great promise for function as the efficient electrocatalysts toward OER, its unfortunately low mass activity and poor electrochemical durability significantly hindered its practical application. To meet the high demand for industrial application, it is highly imperative to promote the OER activity and durability of RuO_2 and RuO_2-based electrocatalysts. This section highlights some advanced strategies for improving the OER performance of RuO_2-based materials, and many advanced RuO_2-based and other nonprecious OER electrocatalysts were summarized in Table 1 (34,37-40,76-84) and Table S1 (Supporting information), respectively.

3.1. Morphology design

In principle, the electrocatalytic performances are correlated with the surface atomic arrangements and electronic configurations of catalysts [85–87]. Therefore, rational morphology design of catalysts could endow them with largely exposed surface active area, which may thus provide more catalytically active sites available for intermediated species, contributing to the large promotion of electrocatalytic activity and long-term stability [88–94]. Many researchers have made lots of efforts to maximize the surface area of RuO_2-based electrocatalysts by rational morphology design. For example, Hu *et al.* have finely controlled the Ru overlayers on the surface of Pd nanosheets [77]. Interestingly, as seen in Figs. 1a and b, the Pd@Ru nanosheets could be transformed into the PdO@RuO_2 heterostructures with ~4 atomic layers of RuO_2 after thermal oxidation treatment. Owing to the unique 2D hexagonal nanosheets structure with abundant surface active sites

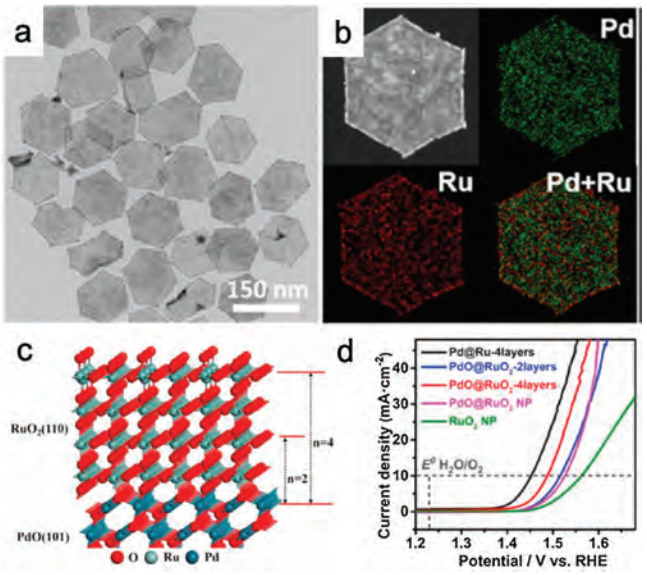

Fig. 1. (a) Transmission electron microscope (TEM) and (b) high-angle annular dark-field scanning transmission electron microscopy (HAADF-STEM) and elemental mapping images of the Pd@Ru. (c) Schematic surface structure of PdO@RuO_2-*n* layers. (d) Linear sweep voltammetry (LSV) curves of different electrocatalysts toward OER in 0.1 mol/L $HClO_4$. Reproduced with permission [77]. Copyright 2019, American Chemica Society.

and weaker bonding of O^* on PdO@RuO_2 to boost the RDS for the generation of HOO^* (Fig. 1c), such PdO@RuO_2 with optimal RuO_2 atomic layer could exhibit high electrocatalytic activity toward OER with the overpotential of only 257 mV at 10 mA/cm^2 (Fig. 1d). More importantly, it was also remarkably to observe that the PdO@RuO_2-4 nanosheets could maintain high activity and nanosheet morphology for even more than 2000 CV cycles, strongly suggesting the outstanding long-term stability.

Very recently, Guo's group have proposed an effective method to fabricate the ultrathin RuRh@(RuRh)O_2 core/shell nanosheets comprised of ultrathin metallic RuRh nanosheets as the core and a few layers of (RuRh)O_2 as the shell [83] (Figs. 2a–d). Remarkably, such ultrathin core/shell nanosheets could display outstanding electrocatalytic OER performance with a low overpotential of 245 mV at 10 mA/cm^2 in 0.1 mol/L $HClO_4$ solution (Fig. 2e). It is interestingly to find that the 2D morphology of ultrathin RuRh@(RuRh)O_2 core/shell nanosheets with high density of surface atoms working as surface active sites guarantee the excellent OER activity and the shell structure of (RuRh)O_2 could effectively lower the fast Ru dissolution of RuRh nanosheets core, thereby contributing to the high electrocatalytic activity and stability. Moreover,

Table 1
Comparison of the activity of RuO_2-based materials for OER.

Catalyst	Electrolyte	Overpotential (mV) @10 mA/cm^2	Mass loading (μg/cm^2)	Ref.
RuO_2	1 mol/L KOH	172	336.9	[34]
RuO_2/CeO_2	1 mol/L KOH	350	280	[37]
Ru@RuO_2	0.5 mol/L H_2SO_4	191	300	[38]
Ru-RuO_2/CNT	1 mol/L KOH	210	800	[76]
2D D-RuO_2/G	0.5 mol/L H_2SO_4	165	140	[39]
Co-RuO_2	0.5 mol/L H_2SO_4	169	–	[40]
PdO@RuO_2	0.1 mol/L $HClO_4$	257	40.0	[77]
Mn-RuO_2	0.5 mol/L H_2SO_4	158	275	[78]
RuO_2@C	0.5 mol/L H_2SO_4	210	5	[79]
NPC@RuO_2	0.5 mol/L H_2SO_4	220	357	[80]
Cu-RuO_2	0.5 mol/L H_2SO_4	188	275	[81]
Co-RuO_2	1 mol/L KOH	200	39.6	[82]
RuRh@(RuRh)O_2	0.1 mol/L $HClO_4$	245	20.4	[83]
$Cr_{0.6}Ru_{0.4}O_2$	0.5 mol/L H_2SO_4	178	283.1	[84]

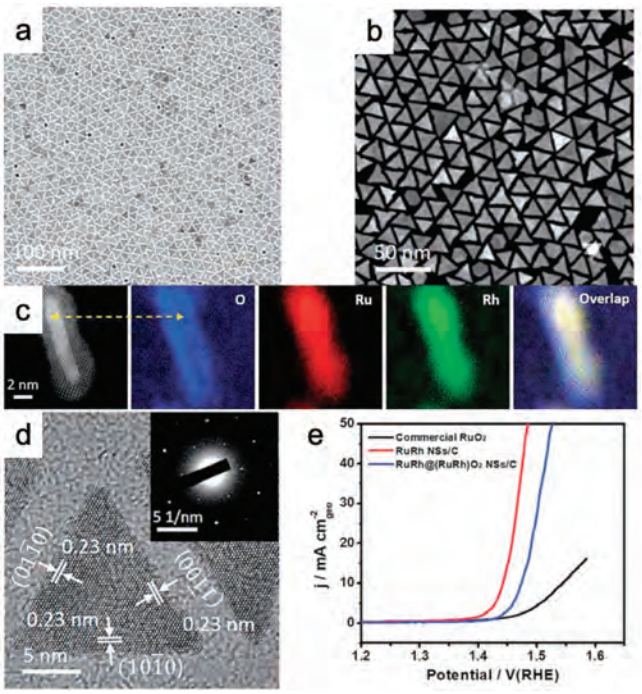

Fig. 2. (a) TEM, (b) HAADF-STEM, (c) elemental mapping, and (d) high resolution TEM (HRTEM) images of the ultrathin RuRh@(RuRh)O_2 core/shell nanosheets. (e) LSV curves of the RuRh@(RuRh)O_2 nanosheets, commercial RuO_2, and RuRh nanosheets in 0.1 mol/L $HClO_4$ solution. Reproduced with permission [83]. Copyright 2020, Royal Society of Chemistry.

theoretical investigations unraveled that the superior OER performances were originated from the electro-activation by the surface oxidation layer, and the shell RuO_2 layer could further pump the electrons toward the adsorbates to effectively facilitate the consecutive reactions during OER process.

In addition to the rational morphology design, it is also a consensus that downsizing the size of a catalyst is also another efficient strategy for promoting the electrocatalytic performance of catalyst. On the one hand, reducing the size of catalyst could help to expose more surface active sites available for intermediates [3,95,96]. On the other hand, introducing appropriate supports to maintain the dispersion of nanoparticles could effectively modify their electronic structure and accelerate the charge transfer, thereby contributing to the large promotion in electroatalytic OER performance [97–99]. Taking inspiration from this, numerous endeavors have been made to improve the electrocatalytic performances of RuO_2-based materials by downsizing them. For instance, Chakraborty *et al.* have synthesized the porous carbon supported RuO_2 nanoparticles with extremely small size (3-4 nm) through a facile self-pyrolysis method employing the covalent organic framework (COF) as a sacrificial precursor [79]. Owing to the high specific surface areas of small-sized RuO_2 nanoparticles and high density of crystallinity of the graphitic sheets, the as-obtained RuO_2@C could catalyze OER with overpotentials of only 210 mV at 10 mA/cm^2 and outstanding electrochemical stability.

3.2. Crystal facet engineering

As previously discussed, the catalytic performance of a catalyst is closely associated with their surface atomic arrangement and configurations [45]. The crystallinity and crystal facet of materials are commonly utilized to regulate the local structure of surface adsorption sites, which plays a crucial role in determining the OER catalytic behaviors [100–103]. For instance, Stoerzinger *et al.* have unraveled that the (100) facet of RuO_2 catalyst is more active in

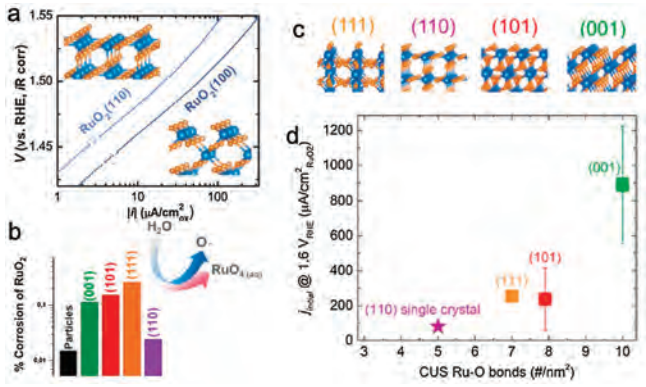

Fig. 3. (a) Tafel plots of RuO_2 (110) and RuO_2 (100). Reproduced with permission [33]. Copyright 2014, American Chemical Society. (b) Histogram of the corrosion of RuO_2 observed in RuO_2 with (111), (110), (101), and (001) surface. (c) Schematics of the (111), (110), (101) and (001) facet and (d) the average current density measured in the 0.05 mol/L H_2SO_4 over 2 h. Reproduced with permission [73]. Copyright 2018, American Chemical Society.

alkaline conditions than the (110) facet for OER due to the richer coordinately unsaturated metal sites on the (100) facet [33] (Fig. 3a). Roy *et al.* have found that the electrocatalytic activity of the prepared thin films with different orientations in 0.05 mol/L H_2SO_4 obeys the order as follows: (001) > (101) > (110) > (111), while the stability is not related to the activity (Figs. 3b–d) [73]. Moreover, Rao *et al.* have declaimed that the deprotonation of OH* intermediates could effectively stabilize OOH* and acted as RDS through density functional theoretical calculation [104].

3.3. Electronic structure engineering

The intrinsic activity of electrochemical reaction is mainly relied on the energy barriers for the adsorption/desorption of intermediated species, governed by the electronic structures of surface active sites [105–110]. Therefore, the catalytic reactivity of catalysts is primarily depended on their surface electronic structures since they are strongly correlated to their electro-catalytic reaction barrier [111]. It has been demonstrated that the reaction barrier energy can effectively be modified by controlling the local electronic distributions of the catalysts, which could tailor the electronic structure whole or in part to promote the catalytic performance [112–116]. To this end, rationally regulating the electronic structure of RuO_2-based materials to reduce their reaction energy barriers is another effective strategy for further promoting their electrocatalytic OER performance. With regard to the electronic structure engineering, doping has been widely considered as an effective way. Chen *et al.* have carried extensive researches on regulating the surface localized electronic structure of RuO_2 by heteroatom doping [78]. For example, they have reported the successful fabrication of Mn-doped RuO_2 nano-crystals *via* annealing the Ru-exchanged Mn-based derivative. Interestingly, the Mn doping in the RuO_2 could effectively regulate the D-band center of Ru active sites and significantly lower the antibonding surface-adsorbate states, which contribute to a decreased free energy of RDS (Fig. 4a), thereby largely promoting the intrinsic activity of RuO_2 (Fig. 4b). Wang *et al.* have developed a general strategy to construct a series of transition metal-doped RuO_2 nanowires with a unique networked structure, abundant surface defects, and plentiful grain boundaries [82] (Fig. 4c). Moreover, the theoretical calculation implied that the D-band center of RuO_2 could be effectively be modified by transition metal doping, which could induce an optimal adsorption energy of intermediates, ultimately contributing to excellent electrocatalytic OER performance (Fig. 4d). As a consequence, the optimal Co-

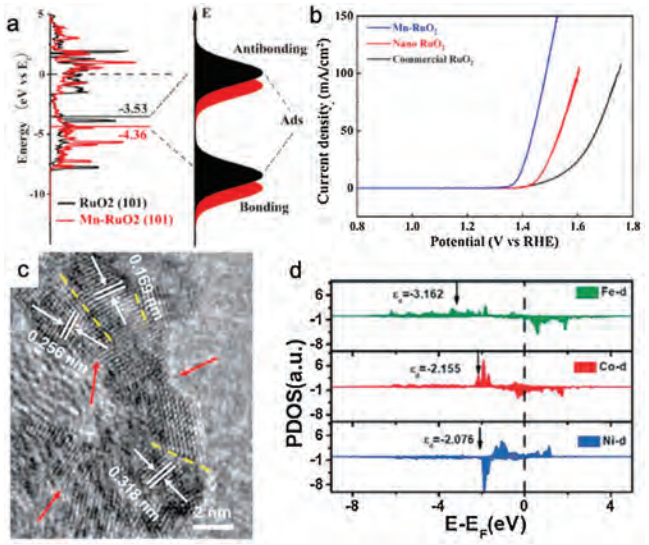

Fig. 4. (a) Calculated density of state of RuO_2, Mn-RuO_2, and the histograms of the antibonding and bonding formation. (b) LSV curves of RuO_2, Mn-RuO_2, and commercial RuO_2. Reproduced with permission [78]. Copyright 2019, American Chemical Society. (c) HRTEM image of the Co-RuO_2. (d) The projected density of state of the Fe, Co, and Ni atoms. Reproduced with permission [82]. Copyright 2019, Royal Society of Chemistry.

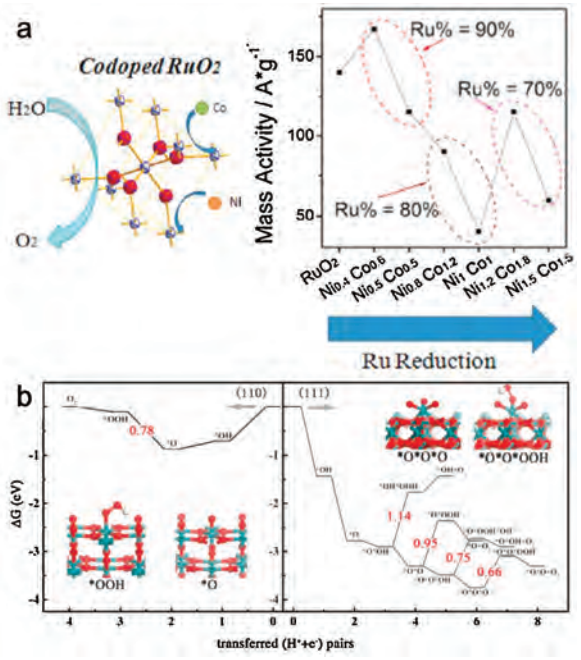

Fig. 5. (a) Schematic illustration of the water oxidation based on Ni-Co codoped RuO_2 and the mass activities of RuO_2 and all codoped composites at the potential of 1.7 V *vs.* RHE. (b) Free energy profile of OER on (110) and (111) surfaces. Reproduced with permission [117]. Copyright 2020, American Chemical Society.

doped RuO_2 nanowires could display remarkable OER activity with the overpotential of 200 mV at 10 mA/cm^2. Su *et al.* have also realized the effective electronic structure engineering of RuO_2 by means of heteroatom doping [81]. Specifically, they have developed a facile approach for the fabrication of Cu-doped RuO_2 hollow polyhedral *via* annealing Ru-exchanged Cu-BTC. Of note, the highly unsaturated Ru sites on the high-index facets could be oxidized to significantly lower the energy barrier of RDS. More importantly, the Cu-dopant could effectively tailor the electronic structures of RuO_2 to further promote their intrinsic OER activity. This work has also demonstrated the synergistic contributions of the surface arrangement and electronic structure engineering.

In addition to the single-doping, dual-doping approaches such as dual-anionic and dual-cationic, have also been well developed to synergistically tune the electronic structures of catalytically active sites. For example, Wu *et al.* have synthesized the Ni-Co codoped RuO_2 nanocatalysts, in which the increase of oxygen vacancies and higher valence of Ru site induced the modification of the host material (Figs. 5a and b), thereby contributing to the outstanding electrocatalytic OER performance [117]. As a result, the codoped RuO_2 with Co/Ni of 1.5 showed high OER kinetic with a Tafel slope of only 32 mV/dec.

3.4. Defect engineering

Besides chemical doping, the electronic structures of the catalytically active sites could also be greatly affected by the surface coordination environments [118,119]. Modifying the crystalline properties of an electrocatalyst could regulate the surface atomic arrangement and coordination environment of the active centers, which could thus significantly promote the electrocatalytic performances of catalysts [120–122]. By creating defects of the catalyst could greatly tailor the surface atomic arrangement and the coordination environment of the catalytically active sites. Generally, owing to the second law of thermodynamics, defects are typically present in all catalysts, which could effectively induce the redistribution of electrochemical property [105,123–126]. To this end, precisely regulating the defects of RuO_2-based materials affords a possibility for improving their electrocatalytic OER performances, and numerous efforts have been made to further promote the electrocatalytic OER performance of the RuO_2 through defect engineering. For example, Li *et al.* have developed a facile finite oxygenation approach to synthesize the defective RuO_2 by employing the oxygen-enriched graphene as the limited oxygen supplier [39] (Fig. 6a). Impressively, the as-prepared defective RuO_2/graphene composite with high specific surface area, abundant hydroxylated surface and intrinsically defective RuO_2 could exhibit extraordinary OER performance with the overpotentials of 169 and 175 mV to achieve 10 mA/cm^2 in acidic and alkaline conditions, respectively (Figs. 6b–d). Moreover, the long-term electrochemical measurements also demonstrated that such defective RuO_2/graphene composite could exhibit excellent long-term electrochemcail stability.

Vacancy, as an intrinsic defect, has also been created to enhance the intrinsic activity of a catalyst [127–129]. In regard to OER, oxygen vacancies in metal oxides have been demonstrated to be crucial for improving their electrocatalytic OER performance [128,130–136]. For example, Wang's group have developed a facile plasma-engraved strategy for creating the oxygen vacancies of Co_3O_4 nanosheets, in which the abundant oxygen vacancies significantly improved the electrocial conductivity of Co_3O_4 as well as provided rich electroactive defects available for intermediated species, thereby contributing to the large enhancement in electrocatalytic OER performance [137]. Taking inspiration from this, Chen's group has synthesized the Co-doped RuO_2 nanorod electrocatalyst enriched with plenty of oxygen vacancies by annealing Ru-exchanged ZIF-67 derivatives [40] (Figs. 7a and b). Remarkably, the abundant oxygen vacancies and modulated electronic structure of the Co-doped RuO_2 nanorod electrocatalyst significantly contributed to greatly improved electrocatalytic OER performance in acidic solution with an overpotential of only 169 mV at 10 mA/cm^2. Theoretical calculations revealed that the OER preferentially proceeded through lattice oxygen oxidation mechanism pathway by passing a lower RDS barrier under the assistance of abundant oxygen vacancies (Figs. 7c and d).

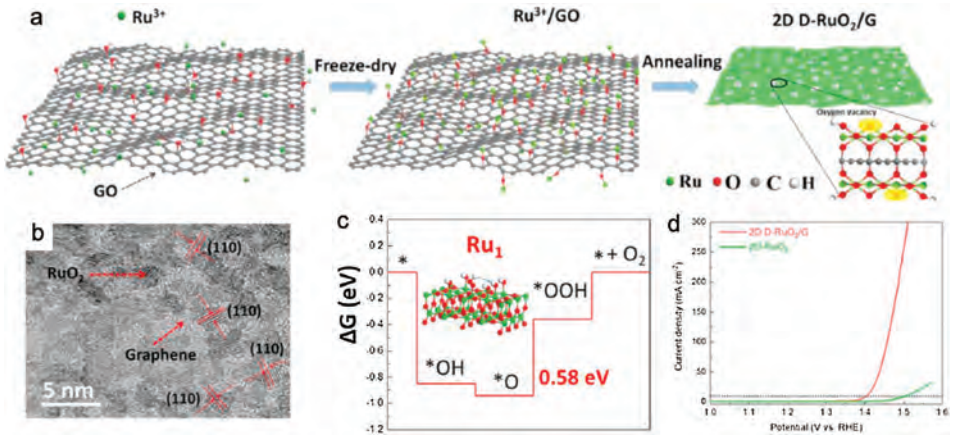

Fig. 6. (a) Schematic illustrating the synthetic process of defective RuO_2/Graphene heterostructures. (b) HRTEM image of the defective RuO_2/Graphene heterostructures. (c) The free-energy profiles of the OER on the Ru site. (d) polarization curves of defective RuO_2/Graphene heterostructures and 2D RuO_2 toward OER. Reproduced with permission [39]. Copyright 2020, Elsevier.

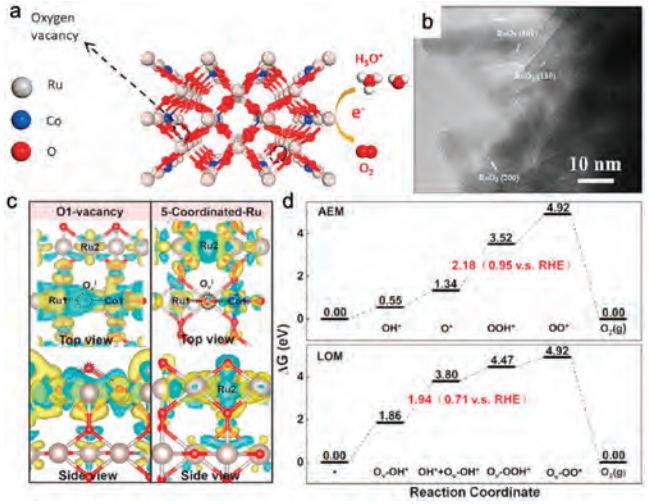

Fig. 7. (a) Schematic and (b) HRTEM image of the Co-doped RuO_2 nanorods. (c, d) Comparison of the OER mechanisms with the different local configurations. Reproduced with permission [40]. Copyright 2020, Elsevier.

3.5. Enhancing conductivity

Considering that the electron transfer rate plays a key role in determining the electrocatalytic activity, constructing a catalyst with high electrical conductivity is highly appreciated [138,139]. For OER electrocatalysts, one of the most effective strategies to improve their electrical conductivity is to introduce appropriate conductive supports [140–142]. Owing to the large surface area, inherent structural stability, and high electrical conductivity, carbon-based nanomaterials have thus been widely utilized as catalyst supports for enhancing the electrical conductivity of the catalysts. For instance, Xie and coworkers have demonstrated the facile synthesis of N-doped CNTs supported RuO_2 nanoparticles (Figs. 8a–c), in which the N-doped CNTs significantly improved the electrical conductivity and structural stability under corrosive conditions [143] (Fig. 8d). More importantly, it is interestingly to find that the nitrogen doping could effectively tailor the electronic structure and electrochemical properties of CNTs, thereby further promoting their electrocatalytic performance (Fig. 8e).

Besides the CNTs, graphene is also an important catalyst support with not only high electrical conductivity but also high specific surface area [124,144,145]. Moreover, the inherently

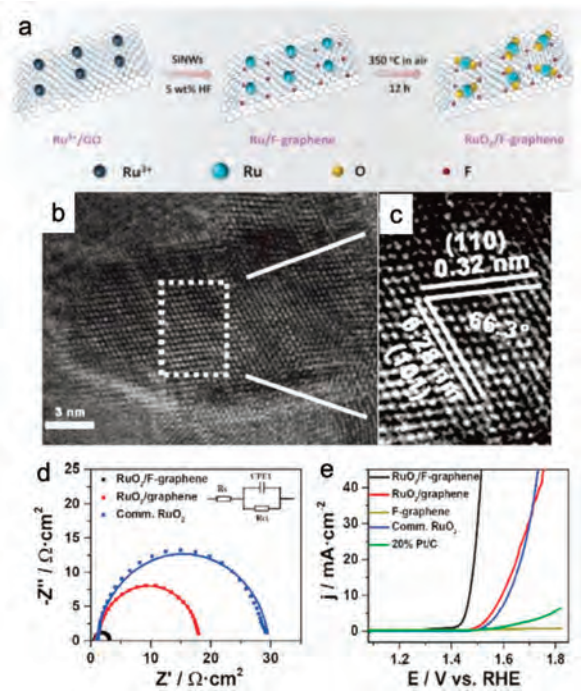

Fig. 8. (a) Schematic illustration of the synthesis process of the RuO_2/F-doped graphene composite. (b, c) HRTEM images of RuO_2/F-doped graphene composite. (d) Nyquist plots of different catalysts in 1 mol/L KOH solution. (e) LSV polarization curves of different catalysts toward OER. Reproduced with permission [146]. Copyright 2020, Royal Society of Chemistry.

mechanical stability also enabled them to be promising supports for electrochemical applications. Inspired by this, Kang's group has utilized the graphene to improve the electrocatalytic OER performance of RuO_2 [146]. To be specific, they have fabricated the RuO_2/F-doped graphene composite, in which the F-doped graphene could help the small RuO_2 nanoparticles to homogeneously distribute without obvious aggregation. Moreover, the addition of fluorine with strong electronegativity could significantly enhance the electrical conductivity and stability of RuO_2/F-doped graphene composite, ultimately leading to the outstanding electrocatalytic OER performance. Consequently, an overpotential of 239 mV is demanded for the RuO_2/F-doped graphene composite

to generate a current density of 10 mA/cm^2 in 1 mol/L KOH solution.

3.6. Heterostructure engineering

Typically, building RuO_2 and other components (*e.g.*, metals, phosphides, sulfides, oxides) into heterostructured composites is also highly favorable for promoting their electrocatalytic activity and durability due to the unique synergistic effect between different components [147]. In addition, the effective electron transfer between different components is also beneficial for further enhancing the electrocatalytic performance of the composites [148–157]. Therefore, building advanced heterostructures offers an effective path to further enhance the electrocatalytic activity and durability of RuO_2-based electrocatalysts through strong synergistic and electronic effect. Taking inspiration from this, Zhang *et al.* have constructed the Ru-RuO_2/CNT hybrids with outstanding electrocatalytic performance for water splitting at a wide range of pH [76]. Comprehensive characterizations coupling with in-depth theoretical studies revealed that metallic Ru, RuO_2 and CNTs synergistically contributed to such high electrocatalytic activity. Moreover, the generated active sites on the interface between Ru and RuO_2 are also favorable for further promoting their electrocatalytic OER performance. Apart from the metal/RuO_2 composites, building RuO_2 with metal oxides is also effective for enhancing their electrocatalytic performance. For example, Galani *et al.* have developed the RuO_2/CeO_2 heterostructure, in which the optimized herterojunction between RuO_2 and CeO_2 facilitated the accumulation of more electrolytes and boosted the electron transportation, potentially leading to the improvements in activity and span of electrocatalysts [37]. As illustrated in Fig. 9a, Chen's group has reported the construction of $Cr_{0.6}Ru_{0.4}O_2$ catalyst derived from metal-organic framework [84]. Comprehensive electrochemical measurements demonstrated that the $Cr_{0.6}Ru_{0.4}O_2$ catalyst could show a record low overpotential of 178 mV at 10 mA/cm^2 in acidic solution (Fig. 9b). Systematical characterizations and in-depth theoretical study demonstrated that the high electrochemical stability was associated with the lower occupation at the Fermi level, while the outstanding electrocatalytic activity was originated from the modified electronic structure by Cr (Fig. 9c). Moreover, the theoretical calculations also demonstrated a low energy barrier for the generation of OOH* (RDS) (Fig. 9d).

Constructing the mixed phases of the Ru-based compounds is also another effective strategy for optimized the activity and stability of the RuO_2 electrocatalyst. Inspired by this, Chorkendorff and coworkers have integrated the advantages of the interface effect with the high anticorrosion ability of IrO_x to construct the IrO_x/RuO_2 heterostructured electrocatalyst [158]. Typically, the sub-monolayers amounts of IrO_x coated at the surface of the RuO_2 greatly protect the Ru against dissolution due to the higher dissolution potential of Ir, leading to the greatly enhanced stability as compared to pure RuO_2 (Fig. 10). Moreover, the strong synergistic effect originated from the heterostructures also contributed to the great promotion of electrocatalytic OER activity, presenting an advanced OER electrocatalyst.

RuO_2, with the favorable bonding energy with oxygen-containing intermediates, has been widely researched as promising electrocatalysts for driving OER. However, the dissolution from the excessive oxidation during OER process made the RuO_2 to be extremely unstable. To overcome these difficulties, considerable endeavors have been made to the design of high-performance RuO_2 electrocatalysts. In a word, we herein highlight the great achievements of the RuO_2-based materials toward OER in alkaline or acidic media. Accordingly to previously advanced researches, the electrocatalytic OER performance of RuO_2 could be significantly improved by morphology design, crystal facet engineering, electronic structure modifications, defect engineering, enhancing conductivity, and heterostructure engineering. For one thing, designing unique morphology could afford abundant surface active sites available for intermediates. For another, the effective electronic structure engineering, defect engineering, and heterostructure engineering could also optimize the bonding energy of oxygen-involved intermediates. These advanced strategies

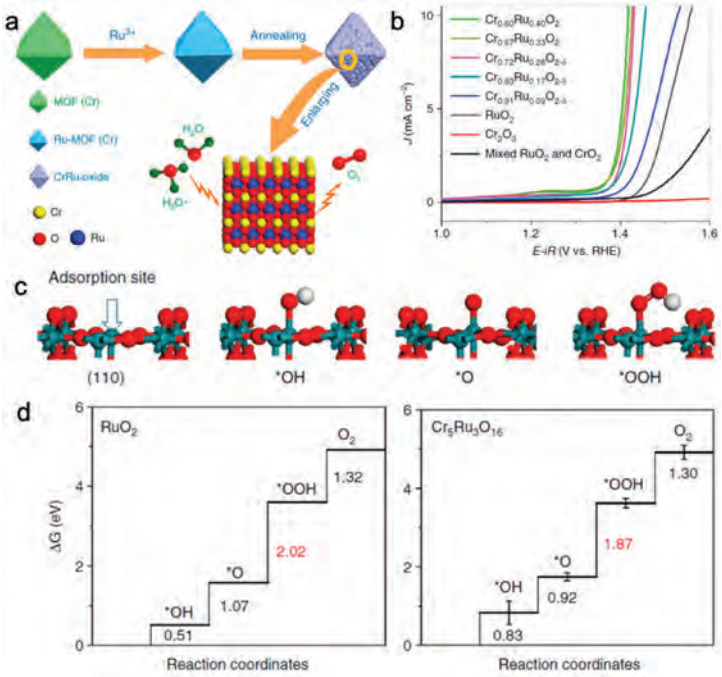

Fig. 9. (a) Schematic illustrating the preparation of the $Cr_{0.6}Ru_{0.4}O_2$ catalysts. (b) OER polarization curves of different catalysts. (c) The four-step OER process based on $Cr_{0.6}Ru_{0.4}O_2$ catalyst. (d) The calculated free energy diagrams for RuO_2 and $Cr_{0.6}Ru_{0.4}O_2$ catalyst. Reproduced with permission [84]. Copyright 2019, Nature Publishing Group.

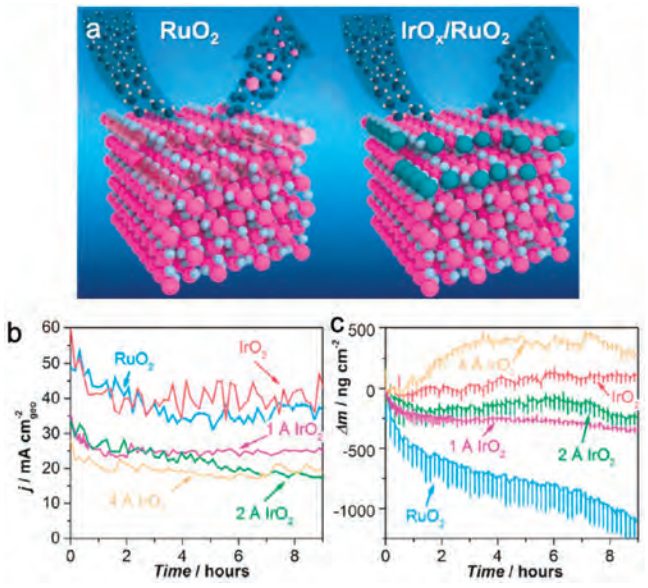

Fig. 10. (a) Schematic illustration of the OER based on pure RuO_2 and IrO_x/RuO_2. (b) Geometric current densities of pure RuO_2 and IrO_x/RuO_2 at 1.8 V (*vs.* RHE) over time and (c) mass loss as a function of time. Reproduced with permission [158]. Copyright 2018, American Chemical Society.

enabled the RuO_2-based electrocatalysts to display promising electrocatalytic performance toward OER.

Although great achievements, there are still many challenges for this flourishing field. (1) Bifunctional properties. Generally, RuO_2-based materials are extensively researched as OER electrocatalysts, while their electrocatalytic performances toward HER are relatively lower, which in turn limited their commercial applications. Therefore, to significantly lower the manufacturing costs, great endeavors should be devoted to the fabrication of RuO_2 electrocatalyst with bifunctional behavior. To address this issue, developing multi-component catalysts by integrating highly active RuO_2 with HER-active components or exploring novel engineering strategies is effective for realizing the bifunctionality. (2) Durability issues. In addition to the reaction kinetics, the long-time stability is also significant for industrial application. It is widely acknowledged that the dissolution from the excessive oxidation during OER process inevitably deactivate the active sites of RuO_2-based materials, resulting in low electrocatalytic activity and poor stability. Therefore, focusing on enhancing the long-time stability of RuO_2-based materials has been of vital significance. Normally, a thorough investigation of the activity degradation *via* advanced techniques is highly urgent, which could offer guidance for the synthesis of more efficient RuO_2-based electrocatalysts. (3) Applicability in a wide pH range. Despite many newly engineering RuO_2-based materials are applicable for OER or HER, while most of the developed RuO_2-based materials for HER-OER bifunctional electrocatalysis could only be performed in basic or acidic media. Nonetheless, such electrolyzers were commonly restrained by many inevitable shortcomings, such as high energy consumption and expensive installation/maintenance. To avoid these problems, exploring and developing highly effective RuO_2-based electrocatalysts in neutral solution is highly sought. (4) Revealing reaction mechanisms. Though many advanced RuO_2-based catalysts are well developed toward OER, the in-depth identifications of the underlying reaction mechanism are still lacking. Therefore, more advanced *in situ* techniques, such as *in situ* transmission electron microscope (TEM), X-ray diffraction (XRD), Raman, and X-ray absorption fine structure (XAFS) should be employed to study the real reaction active sites and atomic-level changes during electrochemical reaction. In addition, closely integrating the systematical characterizations and electrochemical measurements with the theoretical investigations will also better reveal the electrocatalytic processes based on RuO_2-based electrocatalysts.

In a word, RuO_2-based materials showed great promise for the OER, along with the rapid development of material science and the comprehensive understanding of reaction mechanism from atomic level, we believe great opportunity for high-performance OER catalysts and their practical application in energy-conversion techniques will bring a bright prospect in the coming future.

Declaration of competing interest

The authors declare that they have no known competing financial interests or personal relationships that could have appeared to influence the work reported in this paper.

Acknowledgments

We thanked the National Natural Science Foundation of China (Nos. 51873136, 52073199), Natural Science Foundation of the Jiangsu Higher Education Institutions of China (No. 18KJA150008), Natural Science Foundation of Jiangsu Province (No. BK20181428).

Appendix A. Supplementary data

Supplementary material related to this article can be found, in the online version, at doi:https://doi.org/10.1016/j.cclet.2020.11.051.

References

[1] Y. Choi, S.K. Cha, H. Ha, et al., Nat. Nanotechnol. 14 (2019) 245–251.
[2] H. Xu, H. Shang, C. Wang, et al., Adv. Mater. Funct. 30 (2020) 2006317.
[3] Y. Yao, S. Hu, W. Chen, et al., Nat. Catal. 2 (2019) 304–313.
[4] X. Chia, M. Pumera, Nat. Catal. 1 (2018) 909–921.
[5] Z. Xue, X. Li, Q. Liu, et al., Adv. Mater. 31 (2019) e1900430.
[6] A. Li, H. Ooka, N. Bonnet, et al., Angew. Chem. Int. Ed. 58 (2019) 5054–5058.
[7] Y. Lin, Q. Lu, F. Song, et al., Angew. Chem. Int. Ed. 58 (2019) 8917–8921.
[8] P. Xiong, X. Zhang, H. Wan, et al., Nano Lett. 19 (2019) 4518–4526.
[9] X. Gu, Z. Liu, H. Liu, et al., Chem. Eng. J. 403 (2021) 126371.
[10] B. Liu, B. Cao, Y. Cheng, et al., iScience 23 (2020) 101264.
[11] F. Gao, G. Pan, Y. Zhang, et al., Chin. Chem. Lett. 31 (2020) 2230–2234.
[12] H. Wang, S. Zhu, J. Deng, et al., Chin. Chem. Lett. 32 (2021) 291–298.
[13] H. Liu, Z. Liu, F. Wang, et al., Chem. Eng. J. 397 (2020) 125507.
[14] Z. Liu, H. Liu, X. Gu, et al., Chem. Eng. J. 397 (2020) 125500.
[15] P. Han, T. Tan, F. Wu, et al., Chin. Chem. Lett. 31 (2020) 2469–2472.
[16] S. Dutta, C. Ray, Y. Negishi, et al., Chin. Chem. Lett. 30 (2019) 229–233.
[17] L. Feng, R. Ding, Y. Chen, et al., J. Power Sources 452 (2020) 227837.
[18] H. Huang, Y. Zhao, Y. Bai, et al., Adv. Sci. 7 (2020) 2000012.
[19] X. Zhao, J. Meng, Z. Yan, et al., Chin. Chem. Lett. 30 (2019) 319–323.
[20] L. Tian, X. Zhai, X. Wang, et al., J. Mater. Chem. A 8 (2020) 14400–14414.
[21] A. Muthurasu, V. Maruthapandian, H.Y. Kim, Appl. Catal. B: Environ. 248 (2019) 202–210.
[22] Q. Shi, C. Zhu, D. Du, et al., Chem. Soc. Rev. 48 (2019) 3181–3192.
[23] H. Chu, D. Zhang, B. Jin, et al., Appl. Catal. B: Environ. 255 (2019) 117744.
[24] J. Wang, L. Han, B. Huang, et al., Nat. Commun. 10 (2019) 5692.
[25] B. Tang, X. Yang, Z. Kang, et al., Appl. Catal. B: Environ. 278 (2020) 119281.
[26] Q. Xue, W. Gao, J. Zhu, et al., J. Colloid Interface Sci. 529 (2018) 325–331.
[27] M. Yang, T. Feng, Y. Chen, et al., Appl. Catal. B: Environ. 267 (2020) 118657.
[28] Y. Xing, K. Wang, N. Li, et al., Matter 2 (2020) 1494–1508.
[29] H. Sun, J.M. Yang, J.G. Li, et al., Appl. Catal. B: Environ. 272 (2020) 118988.
[30] Z. Zhou, W.Q. Zaman, W. Sun, et al., Chem. Commun. 54 (2018) 4959–4962.
[31] M. Escudero-Escribano, A.F. Pedersen, E.A. Paoli, et al., J. Phys. Chem. B 122 (2018) 947–955.
[32] R.G. González-Huerta, G. Ramos-Sánchez, P.B. Balbuena, J. Power Sources 268 (2014) 69–76.
[33] K.A. Stoerzinger, L. Qiao, M.D. Biegalski, et al., J. Phys. Chem. Lett. 5 (2014) 1636–1641.
[34] Z. Wang, B. Xiao, Z. Lin, et al., J. Energy Chem. 54 (2021) 510–518.
[35] C. Hegde, X. Sun, K.N. Dinh, et al., ACS Appl. Mater. Interfaces 12 (2020) 2380–2389.
[36] J. Chen, H. Li, C. Fan, et al., Adv. Mater. 32 (2020) e2003134.
[37] S.M. Galani, A. Mondal, D.N. Srivastava, et al., Int. J. Hydrogen Energy 45 (2020) 18635–18644.
[38] Y. Wen, T. Yang, C. Cheng, et al., Chin. J. Catal. 41 (2020) 1161–1167.

[39] Y. Li, Y. Wang, J. Lu, et al., Nano Energy 78 (2020) 105185.
[40] Y. Tian, S. Wang, E. Velasco, et al., iScience 23 (2020) 100756.
[41] T. Takashima, K. Hashimoto, R. Nakamura, J. Am. Chem. Soc. 134 (2012) 1519–1527.
[42] Y. Liu, H. Cheng, M. Lyu, et al., J. Am. Chem. Soc. 136 (2014) 15670–15675.
[43] W.D. Chemelewski, J.R. Rosenstock, C.B. Mullins, J. Mater. Chem. A 2 (2014) 14957.
[44] Y. Meng, W. Song, H. Huang, et al., J. Am. Chem. Soc. 136 (2014) 11452–11464.
[45] N. Danilovic, R. Subbaraman, K.C. Chang, et al., J. Phys. Chem. Lett. 5 (2014) 2474–2478.
[46] A. Mendoza-Garcia, H. Zhu, Y. Yu, et al., Angew. Chem. Int. Ed. 54 (2015) 9642–9645.
[47] K. Li, J. Zhang, R. Wu, et al., Adv. Sci. 3 (2016) 1500426.
[48] G. Zhang, G. Wang, Y. Liu, et al., J. Am. Chem. Soc. 138 (2016) 14686–14693.
[49] H. Liang, A.N. Gandi, D.H. Anjum, et al., Nano Lett. 16 (2016) 7718–7725.
[50] M. Liu, J. Li, ACS Appl. Mater. Interfaces 8 (2016) 2158–2165.
[51] P. Chen, K. Xu, T. Zhou, et al., Angew. Chem. Int. Ed. 55 (2016) 2488–2492.
[52] Y. Dou, T. Liao, Z. Ma, et al., Nano Energy 30 (2016) 267–275.
[53] L. Zeng, L. Yang, J. Lu, et al., Chin. Chem. Lett. 29 (2018) 1875–1878.
[54] X. Li, K.-L. Yan, Y. Rao, et al., Electrochim. Acta 220 (2016) 536–544.
[55] J.-H. Zhang, J.-Y. Feng, T. Zhu, et al., Electrochim. Acta 196 (2016) 661–669.
[56] J. Liu, S. Zhao, C. Li, et al., Adv. Energy Mater. 6 (2016) 1502039.
[57] K.R. Yoon, G.Y. Lee, J.W. Jung, et al., Nano Lett. 16 (2016) 2076–2083.
[58] Y. Pi, N. Zhang, S. Guo, et al., Nano Lett. 16 (2016) 4424–4430.
[59] Z. Gao, J. Qi, M. Chen, et al., Electrochim. Acta 224 (2017) 412–418.
[60] M. Gorlin, J. Ferreira de Araujo, H. Schmies, et al., J. Am. Chem. Soc. 139 (2017) 2070–2082.
[61] A. Yu, C. Lee, M.H. Kim, et al., ACS Appl. Mater. Interfaces 9 (2017) 35057–35066.
[62] J. Chi, H. Yu, B. Qin, et al., ACS Appl. Mater. Interfaces 9 (2017) 464–471.
[63] T. Zhang, J. Du, P. Xi, et al., ACS Appl. Mater. Interfaces 9 (2017) 362–370.
[64] A. Nadeema, V.M. Dhavale, S. Kurungot, Nanoscale 9 (2017) 12590–12600.
[65] M. Huynh, C. Shi, S.J. Billinge, et al., J. Am. Chem. Soc. 137 (2015) 14887–14904.
[66] F. Dionigi, T. Reier, Z. Pawolek, et al., ChemSusChem 9 (2016) 962–972.
[67] C. Xie, Y. Wang, D. Yan, et al., Nanoscale 9 (2017) 16059–16065.
[68] P. Cai, J. Huang, J. Chen, et al., Angew. Chem. Int. Ed. 56 (2017) 4858–4861.
[69] J. Yu, G. Li, H. Liu, et al., Adv. Sci. 6 (2019) 1901458.
[70] Y. Li, F. Li, Y. Zhao, et al., J. Mater. Chem. A 7 (2019) 20658–20666.
[71] H. Huang, F. Li, Y. Zhang, et al., J. Mater. Chem. A 7 (2019) 5575–5582.
[72] L. Shi, T. Zhao, A. Xu, et al., ACS Catal. 6 (2016) 6285–6293.
[73] C. Roy, R.R. Rao, K.A. Stoerzinger, et al., ACS Energy Lett. 3 (2018) 2045–2051.
[74] X. Cui, P. Ren, C. Ma, et al., Adv. Mater. 32 (2020) e1908126.
[75] Y. Zhu, X. Ji, C. Pan, et al., Energy Environ. Sci. 6 (2013) 3665.
[76] M. Zhang, J. Chen, H. Li, et al., Nano Energy 61 (2019) 576–583.
[77] Y. Hu, X. Luo, G. Wu, et al., ACS Appl. Mater. Interfaces 11 (2019) 42298–42304.
[78] S. Chen, H. Huang, P. Jiang, et al., ACS Catal. 10 (2019) 1152–1160.
[79] D. Chakraborty, S. Nandi, R. Illathvalappil, et al., ACS Omega 4 (2019) 13465–13473.
[80] J. Yu, G. Li, H. Liu, et al., Adv. Funct. Mater. 29 (2019) 1901154.
[81] J. Su, R. Ge, K. Jiang, et al., Adv. Mater. 30 (2018) e1801351.
[82] J. Wang, Y. Ji, R. Yin, et al., J. Mater. Chem. A 7 (2019) 6411–6416.
[83] K. Wang, B. Huang, W. Zhang, et al., J. Mater. Chem. A 8 (2020) 15746–15751.
[84] Y. Lin, Z. Tian, L. Zhang, et al., Nat. Commun. 10 (2019) 162.
[85] Y. Luo, L. Tang, U. Khan, et al., Nat. Commun. 10 (2019) 269.
[86] W. Zhang, J. Zhao, J. Zhang, et al., ACS Appl. Mater. Interfaces 12 (2020) 10299–10306.
[87] H.F. Wang, L. Chen, H. Pang, et al., Chem. Soc. Rev. 49 (2020) 1414–1448.
[88] S. Hu, Y. Yu, Y. Guan, et al., Chin. Chem. Lett. 31 (2020) 2839–2842.
[89] H. Zhang, J. He, C. Zhai, et al., Chin. Chem. Lett. 30 (2019) 2338–2342.
[90] H. Hu, Bu Y. Guan, Xiong W. Lou, Chem 1 (2016) 102–113.
[91] M. Zhang, J. He, Y. Chen, et al., Chin. Chem. Lett. 31 (2020) 2721–2724.
[92] X.-Y. Yu, Y. Feng, Y. Jeon, et al., Adv. Mater. 28 (2016) 9006–9011.
[93] J. Ding, L. Bu, S. Guo, Nano Lett. 16 (2016) 2762–2767.
[94] Y. Li, Y. Sun, Y. Qin, et al., Adv. Energy Mater. 10 (2020) 1903120.
[95] Z. Li, Y. Chen, S. Ji, et al., Nat. Chem. 12 (2020) 764–772.
[96] Y. Xiong, J. Dong, Z.Q. Huang, et al., Nat. Nanotechnol. 15 (2020) 390–397.
[97] Y. Li, Z.S. Wu, P. Lu, et al., Adv. Sci. 7 (2020) 1903089.
[98] X. Li, X. Yang, Y. Huang, et al., Adv. Mater. 31 (2019) e1902031.
[99] V. Ramalingam, P. Varadhan, H.C. Fu, et al., Adv. Mater. 31 (2019) e1903841.
[100] P.F. Yin, M. Zhou, J. Chen, et al., Adv. Mater. (2020) e2000482.
[101] D. Cao, J. Wang, H. Xu, et al., Small (2020) e2000924.
[102] X. Ma, W. Zhang, Y. Deng, et al., Nanoscale 10 (2018) 4816–4824.
[103] N. Yang, H. Cheng, X. Liu, Adv. Mater. 30 (2018) e1803234.
[104] R.R. Rao, M.J. Kolb, N.B. Halck, et al., Energy Environ. Sci. 10 (2017) 2626–2637.
[105] Y. Li, F.-M. Li, X.-Y. Meng, et al., Nano Energy 54 (2018) 238–250.
[106] E. Cao, Z. Chen, H. Wu, et al., Angew. Chem. Int. Ed. 59 (2020) 4154–4160.
[107] X. Wang, Y. Fei, W. Li, et al., ACS Appl. Mater. Interfaces 12 (2020) 16548–16556.
[108] W. Yang, Z. Wang, W. Zhang, et al., Trends Chem. 1 (2019) 259–271.
[109] C. Wang, H. Xu, Y. Wang, et al., Inorg. Chem. 59 (2020) 11814–11822.
[110] H. Xu, H. Shang, J. Di, et al., Inorg. Chem. 58 (2019) 15433–15442.
[111] E.P. Alsac, E. Ulker, S.V.K. Nune, et al., Chemistry 24 (2018) 4856–4863.
[112] H. Xu, H. Shang, C. Wang, et al., Appl. Catal. B: Environ. 265 (2020) 118605.
[113] Y. Li, Y. Shan, H. Pang, et al., Chin. Chem. Lett. 31 (2020) 2280–2286.
[114] H. Xu, H. Shang, C. Wang, et al., Adv. Funct. Mater. 30 (2020) 2000793.
[115] J.-G. Li, H. Sun, L. Lv, et al., ACS Appl. Mater. Interfaces 11 (2019) 8106–8114.
[116] H. Xu, H. Shang, L. Jin, et al., J. Mater. Chem. A 7 (2019) 26905–26910.
[117] Y. Wu, M. Tariq, W.Q. Zaman, et al., ACS Appl. Energy Mater. 2 (2019) 4105–4110.
[118] H. Xu, H. Shang, C. Wang, et al., Coord. Chem. Rev. 418 (2020) 213374.
[119] H. Xu, P. Song, C. Fernandez, et al., ACS Appl. Mater. Interfaces 10 (2018) 12659–12665.
[120] M. Zhao, Y. Xia, Nat. Rev. Mater. 5 (2020) 440–459.
[121] W. Tong, Q. Shao, P. Wang, et al., Chem. Eur. J. 25 (2019) 7218–7224.
[122] P. Wang, M. Qiao, Q. Shao, et al., Nat. Commun. 9 (2018) 4933.
[123] D. Cao, H. Xu, D. Cheng, Adv. Energy Mater. 10 (2020) 1903038.
[124] Z. Chen, H. Wu, J. Li, et al., Appl. Catal. B: Environ. 265 (2020) 118576.
[125] G. Yilmaz, C.F. Tan, Y.F. Lim, et al., Adv. Energy Mater. 9 (2019) 1802983.
[126] A. Zagalskaya, V. Alexandrov, ACS Catal. 10 (2020) 3650–3657.
[127] N. Zhang, F. Zheng, B. Huang, et al., Adv. Mater. 32 (2020) 1906477.
[128] E. Arciga-Duran, Y. Meas, J.J. Pérez-Bueno, et al., Electrochim. Acta 268 (2018) 49–58.
[129] M.Q. Yang, J. Wang, H. Wu, et al., Small 14 (2018)1703323.
[130] Y. Zhang, J. Fu, H. Zhao, et al., Appl. Catal. B: Environ. 257 (2019) 117899.
[131] Q. Xu, H. Jiang, H. Zhang, et al., Electrochim. Acta 259 (2018) 962–967.
[132] W. Xu, F. Lyu, Y. Bai, et al., Nano Energy 43 (2018) 110–116.
[133] G. Wei, J. He, W. Zhang, et al., Inorg. Chem. 57 (2018) 7380–7389.
[134] Y. Zhao, J. Zhang, W. Wu, et al., Nano Energy 54 (2018) 129–137.
[135] L. Zhuang, L. Ge, Y. Yang, et al., Adv. Mater. 29 (2017) 1606793.
[136] H. Sun, Y. Zhao, K. Molhave, M. Zhang, J. Zhang, Nanoscale 9 (2017) 14431–14441.
[137] L. Xu, Q. Jiang, Z. Xiao, et al., Angew. Chem. Int. Ed. 55 (2016) 5277–5281.
[138] S. Yuan, W. Chen, L. Zhang, et al., Small 15 (2019) e1903311.
[139] E. Detsi, J.B. Cook, B. Lesel, et al., Energy Environ. Sci. 9 (2016) 540–549.
[140] G. Wei, K. Du, X. Zhao, et al., Chin. Chem. Lett. 31 (2020) 2641–2644.
[141] H. Fang, T. Huang, Y. Sun, et al., J. Catal. 371 (2019) 185–195.
[142] H. Xu, B. Yan, S. Li, et al., Chem. Eng. J. 334 (2018) 2638–2646.
[143] K. Xie, W. Xia, J. Masa, et al., J. Energy Chem. 25 (2016) 282–288.
[144] G. Li, J. Wang, J. Yu, et al., Appl. Catal. B: Environ. 261 (2020) 118147.
[145] M. Rahsepar, M.R. Nobakht, H. Kim, et al., Appl. Surf. Sci. 447 (2018) 182–190.
[146] Z. Fan, F. Liao, H. Shi, et al., Inorg. Chem. Front. 7 (2020) 2188–2194.
[147] J. Yu, Q. He, G. Yang, et al., ACS Catal. 9 (2019) 9973–10011.
[148] L. Jin, H. Pang, Chin. Chem. Lett. 31 (2020) 2300–2304.
[149] P. Prabhu, V. Jose, J.M. Lee, Matter 2 (2020) 526–553.
[150] C. Liu, T. Gong, J. Zhang, et al., Appl. Catal. B: Environ. 262 (2020) 118245.
[151] K. Chu, Y.P. Liu, Y.B. Li, et al., Appl. Catal. B: Environ. 12 (2020) 7081–7090.
[152] Y. Liu, S. Jiang, S. Li, et al., Appl. Catal. B: Environ. 247 (2019) 107–114.
[153] B. Wang, C. Tang, H.F. Wang, et al., Adv. Mater. 31 (2019) 1805658.
[154] D. Su, X. Zhang, A. Wu, et al., NPG Asia Mater. 11 (2019) 78.
[155] S. Sun, X. Jin, B. Cong, et al., J. Catal. 379 (2019) 1–9.
[156] H. Xu, P. Song, Y. Zhang, et al., Nanoscale 10 (2018) 12605–12611.
[157] J. Bai, T. Meng, D. Guo, et al., ACS Appl. Mater. Interfaces 10 (2018) 1678–1689.
[158] M. Escudero-Escribano, A.F. Pedersen, E.A. Paoli, et al., J. Phys. Chem. B 122 (2018) 947–955.